Armored Inducible Expression of IL-12 Enhances Antitumor Activity of Glypican-3–Targeted Chimeric Antigen Receptor–Engineered T Cells in Hepatocellular Carcinoma

Ying Liu,* Shengmeng Di,* Bizhi Shi,* Honghong Zhang,† Yi Wang,* Xiuqi Wu,* Hong Luo,* Huamao Wang,† Zonghai Li,*,† and Hua Jiang*

Adoptive immunotherapy based on chimeric antigen receptor–modified T (CAR-T) cells has been demonstrated as one of the most promising therapeutic strategies in the treatment of malignancies. However, CAR-T cell therapy has shown limited efficacy for the treatment of solid tumors. This is, in part, because of tumor heterogeneity and a hostile tumor microenvironment, which could suppress adoptively transferred T cell activity. In this study, we, respectively, engineered human- or murine-derived–armored glypican-3 (GPC3)–specific CAR-T cells capable of inducibly expressing IL-12 (GPC3-28Z-NFAT-IL-12) T cells. The results showed that GPC3-28Z-NFAT-IL-12 T cells could lyse GPC3$^+$ tumor cells specifically and increase cytokine secretion compared with GPC3-28Z T cells in vitro. In vivo, GPC3-28Z-NFAT-IL-12 T cells augmented the antitumor effect when encountering GPC3$^+$ large tumor burdens, which could be attributed to IL-12 increasing IFN-γ production, favoring T cells infiltration and persistence. Furthermore, in immunocompetent hosts, low doses of GPC3-m28Z-mNFAT-mIL-12 T cells exerted superior antitumor efficacy without prior conditioning in comparison with GPC3-m28Z T cells. Also, mIL-12 secretion decreased regulatory T cell infiltration in established tumors. In conclusion, these findings demonstrated that the inducible expression of IL-12 could boost CAR-T function with less potential side effects, both in immunodeficient and immunocompetent hosts. The inducibly expressed IL-12–armored GPC3–CAR-T cells could broaden the application of CAR-T–based immunotherapy to patients intolerant of lymphodepletion chemotherapy and might provide an alternative therapeutic strategy for patients with GPC3$^+$ cancers. ***The Journal of Immunology*****, 2019, 203: 198–207.**

Hepatocellular carcinoma (HCC), an aggressive cancer type, is the fifth most frequent cancer of all malignancies and the third leading cause of cancer-related mortality worldwide (1, 2). Despite the administration of multimodality therapeutic approaches that include curative resection, radiofrequency ablation, transarterial chemoembolization, radioembolization, and systemic targeted agents, like sorafenib, the late stage of patient presentation and the high rate of recurrence have caused unfavorable prognosis (3, 4). This highlights the need to develop an effective, life-prolonging therapeutic modality for patients suffered from HCC.

Adoptive immunotherapy by genetically engineering lymphocytes to use chimeric antigen receptor–modified T (CAR-T) cells has been demonstrated as a promising treatment of malignant diseases in recent years (5). Traditional CARs are composite, artificial antigen receptors, commonly composed of an extracellular recognition domain, a TCR-derived CD3ζ domain, and one or more intracellular costimulatory domains. The adoptive transfer of T cells modified with a CD19-specific CAR has demonstrated remarkable success in treating patients with B cell lymphoid malignancies (6–9). However, attempts to recapitulate the success achieved with CAR-T cells in B cells malignancies for solid tumors have been unsatisfactory (10–14). One of main impediments encountered for the application of CAR-T cell therapies for solid tumors is the immunosuppressive effect of the tumor microenvironment (15). Many improvements have been made to the CAR design in improving the antitumor efficacy of CAR-T cells. Genetic modifications to CAR constructs with proinflammatory cytokines have also been described (16, 17). These armored CAR-T cells have been engineered to secrete cytokines to further enhance CAR-T cell efficacy. Among these cytokines, one promising candidate is IL-12.

IL-12 is a proinflammatory cytokine that bridges innate and adaptive immunity (18), and it exhibits pleiotropic biological effects, including enhancing the function of NK cells and CTLs, promoting secretion of IFN-γ, favoring the generation of CD4$^+$ Th1 cells, as well as reprogramming myeloid-derived suppressor cells (19–22). A series of preclinical researches in murine tumor models have demonstrated the antitumor activity of rIL-12 by regressing tumors or prolonging the survival of tumor-bearing animals (23). Nevertheless, systemic use of IL-12 in clinical trials caused severe unexpected side effects, which extremely limits its clinical application (24, 25). To date, several preclinical studies have also demonstrated the enhanced antitumor activity

*State Key Laboratory of Oncogenes and Related Genes, Shanghai Cancer Institute, Renji Hospital, Shanghai Jiaotong University School of Medicine, Shanghai 200032, China; and †CARsgen Therapeutics, Shanghai 200233, China

ORCIDs: 0000-0003-2448-3636 (Z.L.); 0000-0001-8328-339X (H.J.).

Received for publication January 9, 2018. Accepted for publication April 28, 2019.

This work was supported by the National Natural Science Foundation of China (81871918 and 81872483), the Shanghai Municipal Commission of Health and Family Planning (201740124), the "13th Five-Year Plan" National Science and Technology Major Project of China (2017ZX10203206006001), and the seed fund of Renji Hospital (RJZZ17-021).

Address correspondence and reprint requests to Dr. Hua Jiang and Dr. Zonghai Li, State Key Laboratory of Oncogenes and Related Genes, Shanghai Cancer Institute, Renji Hospital, Shanghai Jiaotong University School of Medicine, No. 25/Ln2200 Xie Tu Road, Shanghai 200032, China. E-mail addresses: jianghuapy@163.com (H.J.) and zonghaili@shsmu.edu.cn (Z.L.)

The online version of this article contains supplemental material.

Abbreviations used in this article: CAR-T, chimeric antigen receptor–modified T; GPC3, glypican-3; GPC3-28Z-NFAT-IL12, inducible IL-12–secreting CAR; HCC, hepatocellular carcinoma; hscIL-12, human single-chain IL-12; IHC, immunohistochemistry; mUTD, murine UTD; scFv, single-chain variable fragment; Treg, regulatory T cell; UTD, untransduced T.

of CAR-T cells secreting IL-12 constitutively or inducibly against ovarian tumors and melanoma (26, 27).

Glypican-3 (GPC3) is a membrane protein and overexpressed in most HCC but not nonmalignancies, including normal or cirrhotic liver (28). Several clinical trials have proved targeting GPC3 is safe and well tolerated (29–31). In our phase I clinical trial of anti-GPC3 CAR-T cells in 13 patients with refractory or relapsed $GPC3^+$ HCC, five patients infused with anti-GPC3 CAR-T cells without lymphodepleting conditioning developed progressive disease shortly after CAR-T therapy. Among eight patients in another group, who received lymphodepletion treatment with fludarabine and cyclophosphamide before anti-GPC3 CAR-T cells transfusion, one patient achieved partial response (32). Although these results demonstrated that the anti-GPC3 CAR-T cell was safe and well tolerated, the antitumor efficacy was not potent enough. The adverse factors involved in impeding CAR-T–based immunotherapy may be attributed to the heterogeneity of tumor cells and the suppression of tumor microenvironment. Given the safety showed by our anti-GPC3 CAR-T cells in phase I clinical trial and the exclusive expression of GPC3 in malignancies (33), it provided us with a rationale to enhance the therapeutic efficacy by exploring the potential of anti-GPC3 CAR-T cells modified to deliver therapeutic cytokines to the tumor environment.

Therefore, in this study, we investigated the feasibility of targeted delivery of IL-12 to tumor sites through infusion of anti-GPC3 CAR-engineered T cells expressing IL-12. To avoid cell toxicity associated with constitutive expression of IL-12, inducible IL-12–secreting CARs (GPC3-28Z-NFAT-IL-12) were developed, and an NFAT-responsive promoter was used to restrict the expression of IL-12 to activated T cells triggered by specific tumor Ag recognition. Our results demonstrated that anti-GPC3 CAR-T cells engineered to inducibly expressing IL-12 enhanced the therapeutic effect in $GPC3^+$ HCC-established tumor models of immunodeficient and immunocompetent mice.

Materials and Methods

Cell lines and culture

The human HCC cell lines PLC/PRF/5 and SK-HEP-1 and the human embryonic kidney (HEK)–293T cell line were purchased from the American Type Culture Collection. The human HCC cell line Huh-7 was obtained from the RIKEN BRC Cell Bank. The murine HCC cell line Hepa1-6 was purchased from the Chinese Academy of Sciences (Shanghai, China). Hepa1-6-GPC3 (Hepa1-6 cells with human mouse chimeric GPC3 overexpression) was established and conserved by our laboratory. All the cell lines mentioned above were cultured in DMEM (Life Technologies) supplemented with 10% FBS (Life Technologies) and 100 U/ml penicillin and 100 μg/ml streptomycin (Life Technologies). Human PBMCs derived from healthy human donors were obtained from the Shanghai Blood Center. Human PBMCs and human T cells were cultured in AIM-V Medium CTS (Life Technologies) supplemented with 2% human AB serum (Gemini Bio-Products) and 500 IU/ml recombinant human IL-2 (Shanghai Huaxin High Biotechnology). Murine $CD3^+$ T cells were isolated from murine splenocytes derived from C57BL/6 using a mouse T cell isolation kit (STEMCELL Technologies) and cultured in RPMI 1640 supplemented with 10% heat-inactivated FBS, 50 μM 2-ME, 100 U/ml penicillin, 100 μg/ml streptomycin, and 100 IU/ml of recombinant human IL-2. All the cells were cultured at 37°C in a 5% CO_2 incubator.

CARs construction

All lentivirus and retroviral vector constructs used in this study are schematically illustrated in Figs. 1A and 5A. The second generation of the GPC3-specific CAR, named GPC3-28Z, comprised the anti-GPC3 single-chain variable fragment (scFv) (34) linked in-frame to the human CD8α hinge, which fused to the human CD28 molecule transmembrane region and the intracellular signaling domains and CD3ζ molecules, which were amplified by PCR from another anti-GPC3 CAR in our laboratory (35). GPC3-28Z was cloned into MluI/SalI sites of a lentiviral pRRLSIN vector backbone (36). GPC3-28Z-NFAT-IL-12 was generated by fusing GPC3-28Z with a human $NFAT_6$-IL-12-PA2 cassette, which was composed of six repeats of human NFAT-binding motif, a human minimal IL-2 promoter, and a human single-chain IL-12 (hscIL-12) as well as a Poly(A) signal sequence (PA2) (37, 38). The hscIL-12 was designed by connecting the human IL-12 p40 and human IL-12 p35 subunits with a $(Gly_4Ser)_3$ linker (39). Similarly, the second generation of the murine GPC3-specific CAR, named GPC3-m28Z, consists of an anti-GPC3 scFv (34) linked in-frame to the hinge and transmembrane regions of the murine CD8α-chain, which in turn fused to the murine CD28 intracellular signaling sequences, and murine CD3ζ molecules (40). GPC3-m28Z was cloned into EcoRI/SalI sites of the MSCV-IRES-GFP (Addgene). To generate murine IL-12–armored murine anti-GPC3 CAR, named GPC3-m28Z-mNFAT-mIL-12, the GPC3-28Z was fused with a murine $NFAT_6$-IL-12-PA2 cassette, which consisted of six repeats of murine NFAT-binding motif, a murine minimal IL-2 promoter, and a murine single-chain IL-12 as well as a PA2 in tandem (37, 38). The murine single-chain IL-12 was generated by fusing the murine IL-12p40 and murine IL-12p35 subunits with a $(Gly_4Ser)_3$ linker.

Lentivirus and retrovirus production

For lentivirus production, the 293T cells were seeded at 1.5×10^7 per 15-cm dish before transduction. On the next day, 293T-cells were transfected with the different recombinant CAR expression vectors encoding GPC3-28Z and GPC3-28Z-NFAT-IL-12 in addition to the lentiviral packaging plasmid pMDLg/pRRE, pRSV-Rev, and envelope-expressing plasmid pCMV-VSV-G (Addgene) by using a polyethyleneimine-based DNA transfection reagent (41, 42), and the medium was replaced 6 h later. The viral supernatants were harvested at 48 or 72 h after transfection. The lentiviral particles were concentrated 50-fold by polyethylene glycol (Sigma-Aldrich). For retrovirus production, the 293T cells were seeded at 1.5×10^7 per 15-cm dish. On the next day, 293T cells were transfected with the different recombinant murine CAR expression vectors encoding GPC3-m28Z and GPC3-m28Z-mNFAT-mIL-12 together with the retroviral packaging plasmid pCL-Eco (Addgene) by using a polyethyleneimine-based DNA transfection reagent (41, 42). Also, the medium was changed 6 h later. The viral supernatants were harvested at 48 h after transfection.

Transduction of T cells

Human PBMCs were activated with anti-CD3/anti-CD28–coated magnetic beads (Invitrogen) on day 0. Forty-eight hours later, T cells were then transduced with concentrated lentiviruses on 24-well plates coated with RetroNectin (Takara Bio) in the presence of polybrene (Polysciences). Similarly, mouse $CD3^+$ T cells were stimulated with anti-mouse CD3/anti-mouse CD28 magnetic beads (Life Technologies) for 24 h, and then transduced with retroviruses on RetroNectin-coated 24-well plates. The transduced human and mouse T cells were fed with fresh medium every other day.

Flow cytometry

The detection of GPC3 expression has been previously described (43). CAR expression was detected by staining T cells with goat anti-human IgG, $F(ab')_2$ fragment–conjugated biotin (Jackson ImmunoResearch), followed by streptavidin-PE (eBioscience). In addition, the amounts of circulating human T cells in peripheral blood from tumor-bearing mice treated with CAR-T cells were quantified by the CD3-PerCP/CD4-FITC/CD8-PE Trucount kit (BD Biosciences). Intracellular stain with murine IL-12–eFluor 488 (eBioscience) was performed to detect mIL-12. The fluorescence was analyzed using a BD FACSCelesta Flow cytometer, and the data were analyzed using FlowJo 7.6 software.

Western blot

To confirm the expression of CAR protein in transduced T cells, T cells were lysed with lysis buffer for 1 h on ice. Subsequently, cell lysate was removed by centrifugation at $12{,}000 \times g$ for 10 min. Samples were electrophoresed by a 10% SDS-PAGE gel and transferred to a nitrocellulose membrane. Next, the nitrocellulose membrane was immunoblotted with a mouse anti-human CD3ζ Ab (BD Biosciences), followed by incubation with HRP-conjugated rabbit anti-mouse IgG (H&L) (KangChen Biotech). Finally, the expression of CD3ζ was detected by the ECL Western blot analysis system (Pierce).

Cytotoxicity assays

Different target cancer cells were cocultured with the CAR-T cells at effector/target ratio of 3:1, 1:1, and 1:3. Following 18 h of coculture, the levels of supernatant lactate dehydrogenase were tested by the CytoTox 96 Non-Radioactive Cytotoxicity Kit (Promega) in accordance with the manufacturer's instructions.

Cytokine release assays

Both human and mouse T cells were cocultured with target tumor cells at a 1:1 ratio. 24 h later, supernatant was collected. Mouse T cells were stimulated with 10 μg/ml Concanavalin A (Sigma-Aldrich) overnight, followed by supernatant collection. The levels of human and murine IL-2, IFN-γ, TNF-α, and IL-12p70 secreted, respectively, by human and mouse T cells were detected by using a commercially available ELISA kit (MultiSciences Biotech) according to the manufacturer's manual. For serum cytokine release assay, mouse sera were collected by centrifuging peripheral blood at 1000 × *g* for 30 min and then measured by ELISA kits.

Immunohistochemistry assays

All samples for immunohistochemistry (IHC) assays were fixed with formalin and embedded in paraffin. Next, serial sections were performed. To detect human $CD3^+$ T cells, the sections of formalin-fixed, paraffin-embedded tumor tissue and livers from mice treated with human T cells were immunostained with anti-CD3ε Ab (Thermo-Fisher Scientific) followed by peroxidase-conjugated secondary Abs (ChemMate Dako Envision Detection Kit, Peroxidase/DAB, Rabbit/Mouse; Dako). A normal rabbit IgG served as an isotype-matched control. Briefly, after deparaffinization and blocking of endogenous peroxidase, Ag retrieval was achieved by microwave using sodium citrate solution (pH 6). Subsequently, the slices were blocked in BSA (1%) for 30 min at room temperature and immunostained with anti-CD3ε Ab at 1:500 dilution overnight at 4°C. Next, the sections were washed with PBS and incubated with peroxidase-conjugated secondary Abs for 1 h and counterstained with hematoxylin. To detect murine $CD8^+$ T cells and regulatory T cells (Tregs), the sections of formalin-fixed, paraffin-embedded tumor tissue were immunostained with anti-mouse CD8α Ab (Cell Signaling Technology) or anti-mouse Foxp3 mAb (eBioscience), followed by goat anti-rat IgG-HRP (Santa Cruz Biotechnology) or HRP-conjugated rabbit anti-mouse IgG (H&L) (KangChen Biotech). The IHC staining procedures were similar to the procedure described above.

Real-time PCR

Genomic DNA from tumor tissues was purified using a QIAamp DNA Mini Kit (QIAGEN) in accordance with the manufacturer's handbook. The CAR copy number was measured by quantitative real-time PCR and normalized by simultaneous measurement of the plasmid encoding GPC3-m28Z using TaqMan Fast Advanced Master Mix (Thermo-Fisher Scientific). The forward primer sequences 5′-GACGTTGGGTTACCTTCTGC-3′ and reverse primer sequence 5′-TTCCCAGGTCACGATGTAGG-3′ were used to amplify a CAR sequence. The TaqMan probe sequence is 5′-ATGGCCGCGAGACGGCACCT-3′.

Xenograft tumor models

For the established PLC/PRF/5 xenograft tumor models, 6-wk-old female NSG mice were inoculated s.c. with 3×10^6 PLC/PRF/5 cells on the right flank. When the tumor lesions were ∼250–300 mm^3 in vol, animals were randomly divided into three groups ($n = 6$) and subsequently injected i.v. with the indicated CAR-T cells (3×10^6 CAR-T cells per mouse). For the established Huh-7 xenograft tumor models, 6-wk-old female NSG mice were challenged s.c. with 2×10^6 Huh-7 cells on the right flank. When the tumor volumes were ∼600–650 mm^3, animals were randomly divided into three groups ($n = 6$) and subsequently injected i.v. with the indicated CAR-T cells (3×10^6 CAR-T cells per mouse). To establish Hepa1-6-GPC3 models, 6-wk-old female C57BL/6 mice were inoculated with 1×10^7 Hepa1-6-GPC3 cells on the right flank. And when tumor burdens were 300–350 mm^3, respectively, mice were randomly allocated into four groups ($n = 6$), followed by injection with indicated murine CAR-T cells. Tumor dimensions were measured by Vernier calipers every 3–4 d, and tumor volumes were calculated using the following formula: $V = (\text{length} \times \text{width}^2) \div 2$. All animals were housed and treated under specific pathogen–free conditions, and all experiments were carried out according to protocols approved by the Shanghai Medical Experimental Animal Care Commission.

Statistical analysis

All data are presented as the mean ± SEM. Statistical analysis was performed using two-way ANOVA with Bonferroni posttest or Student *t* test for two-sample comparisons. GraphPad Prism 5.0 was used for statistical calculations, and $p < 0.05$ (*), $p < 0.01$ (**), and $p < 0.001$ (***) were considered significant.

Results

Generation of GPC3-specific CAR-T cells releasing inducible IL-12

The schematic representation of the lentiviral vector constructs used in this study is shown in Fig. 1A. A second generation CAR targeting to GPC3 (GPC3-28Z) using a mAb specific for GPC3 Ag was constructed (34). And the GPC3-28Z construct was further modified to express the hscIL-12 under the transcriptional control of NFAT-responsive minimal IL-2 promoter that drives IL-12 expression only in activated T cells (37), designated as GPC3-28Z-NFAT-IL-12 (Fig. 1A). CD3/CD28–activated human PBMCs from healthy donors were transduced with lentiviruses encoding GPC3-28Z or GPC3-28Z-NFAT-IL-12 constructs, and the

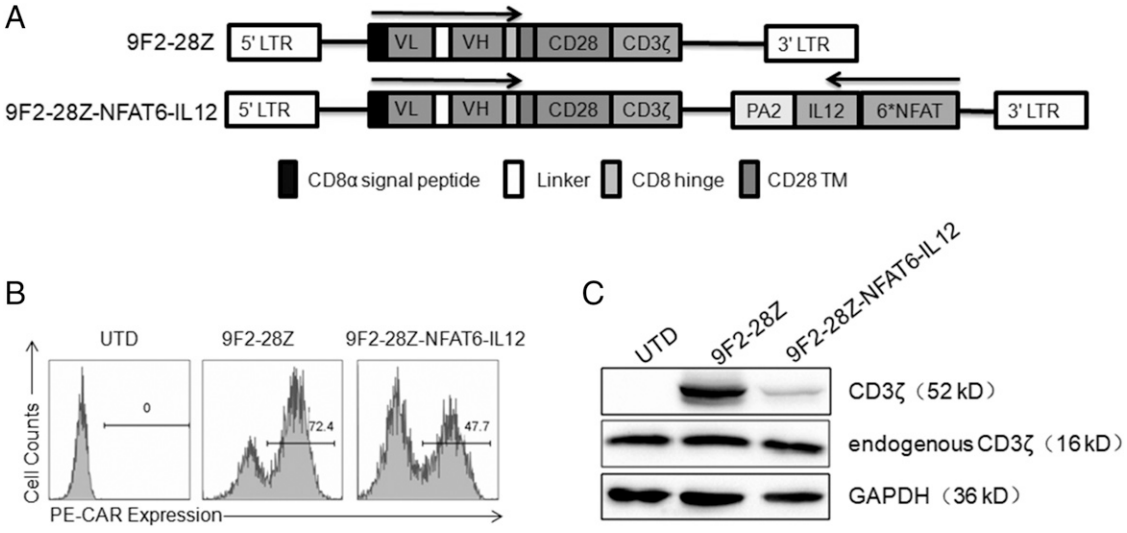

FIGURE 1. Construction of GPC3-28Z-NFAT-IL-12 T cells. (**A**) Schematic representation of GPC3-specific CAR (GPC3-28Z) and GPC3-28Z-NFAT-IL-12. (**B**) GPC3-CARs expression on human T cells transduced with lentiviruses encoding GPC3-28Z or GPC3-28Z-NFAT-IL-12 was detected by FACS. Untransduced T (UTD) cells were used as controls. (**C**) Western blot analysis of the CAR expression. A goat anti-human CD3ζ Ab was used to demonstrate the endogenous and chimeric CD3ζ proteins. The GAPDH served as a loading control.

untransduced T (UTD) cells were used as controls. On day 7 after transduction, the expression of CARs in the transduced T cells was measured by FACS analysis (Fig. 1B). CARs expression was also confirmed by Western blotting with anti-CD3ζ Ab (Fig. 1C).

Activation-dependent IL-12 secretion and in vitro function of GPC3-28Z-NFAT-IL-12 T cells

To verify whether the secretion of bioactive IL-12 in GPC3-28Z-NFAT-IL-12 T cells is dependent on CAR engagement of GPC3$^+$ tumor cells, three HCC cell lines were chosen. These cells expressed various levels of GPC3 confirmed by FACS analysis. Huh-7 had the higher GPC3 expression level than PLC/PRF/5, whereas SK-HEP-1 had no GPC3 expression (Fig. 2A). As expected, neither GPC3-28Z T cells cocultured with GPC3$^+$ tumor cells nor GPC3-28Z-NFAT-IL-12 T cells cocultured with GPC3-negative tumor cells could release IL-12 at detectable levels. Only GPC3-28Z-NFAT-IL-12 T cells cocultured with GPC3$^+$ tumor cells produced a significantly high level of IL-12 (Fig. 2B), which demonstrated that GPC3-28Z-NFAT-IL-12 T cells were able to release IL-12 in an Ag-restricted manner. To explore the bioactivity of IL-12 displayed on CAR-T cells, we detected the cytokine production of GPC3-28Z-NFAT-IL-12 and GPC3-28Z T cells when cocultured with tumor cells. The amount of IFN-γ was increased significantly in GPC3-28Z-NFAT-IL-12 T cells in comparison with GPC3-28Z T cells when cocultured with GPC3$^+$ tumor cells (Fig. 2C). We also found elevated IL-2 and TNF-α production in GPC3-28Z-NFAT-IL-12 T cells when cocultured with PLC/PRF/5 but not Huh-7 cells in comparison with GPC3-28Z T cells, indicating the different characteristic between cell lines. Further, the cytotoxicity assays were performed by incubating T cells against various HCC cells. The results illuminated that both GPC3-28Z T cells and GPC3-28Z-NFAT-IL-12 T cells could specifically lyse GPC3$^+$ target cells with equally efficiency (Fig. 2D). These results suggested that genetic modification of T cells with GPC3-28Z-NFAT-IL-12 did not affect the cytolysis ability.

Improved antitumor activity of GPC3-28Z-NFAT-IL-12 T cells against established HCC xenografts with low or high GPC3 expression

The transferred human T cells were infused into NSG mice bearing s.c.-established PLC/PRF/5 xenografts when tumors grew to 250–300 mm^3 (Fig. 3A). As shown in Fig. 3A, 3×10^6 GPC3-28Z-NFAT-IL-12 T cells mediated extraordinary inhibition of tumor growth, whereas UTD and GPC3-28Z T cells were unable to suppress tumor growth. The tumor-inhibiting rates of GPC3-28Z– and GPC3-28Z-NFAT-IL-12 T cells–treated group were 11 and 95%, respectively, 23 d after T cell injection (Fig. 3B). In addition, mice body weight was also monitored simultaneously. The data showed that there was no significant body weight loss in mice treated with GPC3-28Z-NFAT-IL-12 T cells compared with other groups (Fig. 3C). To elucidate the mechanism of the antitumor function of GPC3-28Z-NFAT-IL-12 T cells, we assessed the secretion of IFN-γ and IL-12 (p70) in the sera of mice. As shown in Fig. 3D, elevated levels of serum IFN-γ and IL-12 were detected in mice treated with GPC3-28Z-NFAT-IL-12 T cells in contrast with mice treated with GPC3-28Z T cells.

We further explored the antitumor efficiency of GPC3-28Z-NFAT-IL-12 T cells in NSG mice bearing Huh-7 xenografts, which was high endogenous GPC3 expression. Mice bearing large tumor xenografts were treated with 3×10^6 T cells when

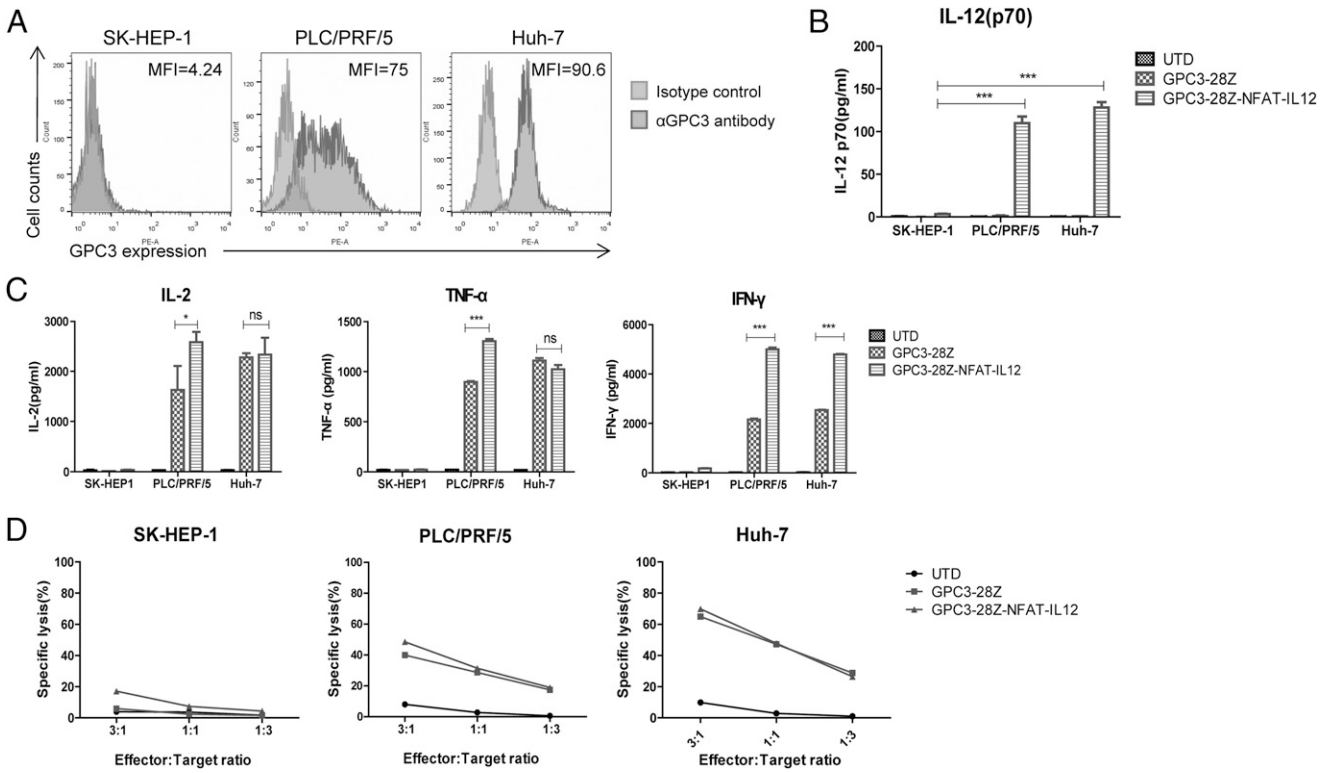

FIGURE 2. Activation-dependent IL-12 production and in vitro function of GPC3-28Z-NFAT-IL-12 T cells. (**A**) Surface GPC3 expression (black) on HCC cell lines was detected by FACS. Isotype Ab served as a control. (**B** and **C**) The secretion of bioactive IL-12p70, IL-2, TNF-α, and IFN-γ of T cells following 24 h coculture with HCC cells at 1:1 ratio was determined by ELISA. Data shown are the mean ± SEM of triplicates. (**D**) In vitro cytotoxicity of T cells incubated with indicated target cells at 3:1, 1:1, and 1:3 ratios for 18 h. Each data set reflects mean ± SEM of quintuplicate. *$p < 0.05$, ***$p < 0.001$.

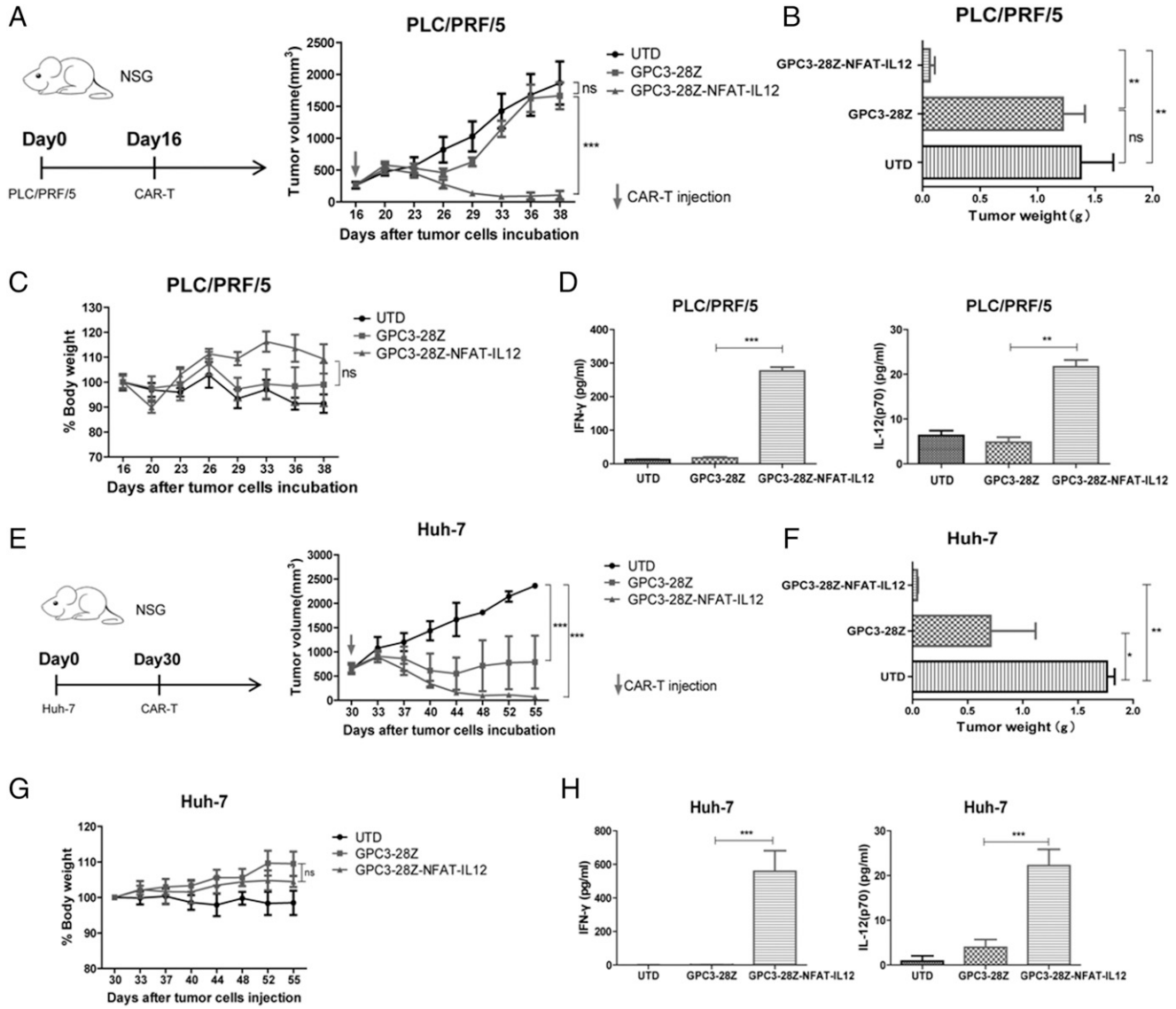

FIGURE 3. Improved antitumor efficacy of GPC3-28Z-NFAT-IL-12 T cells against GPC3-expression tumor xenografts. A total of 3×10^6 PLC/PRF/5 or 2×10^6 Huh-7 cells were inoculated on the right flank of 6-wk-old female NSG mice on day 0. (**A**) Left panel, Experimental scheme of in vivo therapeutic efficacy experiment. On day 16, mice bearing tumors of ~250–300 mm^3 were infused i.v. with 3×10^6 indicated T cells ($n = 6$). Right panel, Growth curve of PLC/PRF/5 xenografts treated with indicated T cells. Arrow indicates T cells infusion. (**B** and **F**) The tumor weight was measured at the study end point. (**C** and **G**) Body weight of each group was measured every 3–4 d (baseline = 100%). (**D**) The amount of IFN-γ and IL-12 in the sera of treated mice 23 d after T cells infusion was measured by ELISA. Data shown are the mean ± SEM from three mice of each group. (**E**) Left panel, Experimental scheme of in vivo antitumor experiment. On day 30, mice bearing tumors of ~600–650 mm^3 were infused i.v. with 3×10^6 indicated T cells ($n = 6$). Right panel, Growth curve of Huh-7 xenografts treated with indicated T cells. (**F**) The amount of IFN-γ in the sera of treated mice 10 d after T cell infusion was measured by ELISA. Data shown are the mean ± SEM from three mice of each group. (**H**) The amount of IFN-γ and IL-12 in the sera of treated mice 10 d after T cell infusion was measured by ELISA. Data shown are the mean ± SEM from three mice of each group. $*p < 0.05$, $**p < 0.01$, $***p < 0.001$.

tumor volume grew to 650–700 mm^3. As shown in Fig. 3E, GPC3-28Z-NFAT-IL-12 T cells significantly suppressed the tumor growth compared with the control groups. The tumor-inhibiting rates of GPC3-28Z and GPC3-28Z-NFAT-IL-12 T cell groups were 59 and 98%, respectively, 25 d after T cell infusion (Fig. 3F). Likewise, no significant body weight loss and pathological changes in organs of mice treated with GPC3-28Z-NFAT-IL-12 T cells were observed (Fig. 3G, Supplemental Fig. 1A). Serum IFN-γ and IL-12 (p70) levels were then measured. As shown in Fig. 3H, mice treated with GPC3-28Z-NFAT-IL-12 T cells manifested significantly elevated levels of serum IFN-γ and IL-12 in contrast with mice treated with GPC3-28Z T cells.

In vivo persistence and infiltration of GPC3-28Z-NFAT-IL-12 T cells

The CAR-T cells persistence in peripheral blood of treated mice was further determined. For PLC/PRF/5 and Huh-7 xenografts models, the peripheral blood of mice treated with GPC3-28Z-NFAT-IL-12 T cells had significantly more human T cells than that of GPC3-28Z T cells 14 d after T cell infusion (Fig. 4A, 4C). Furthermore, IHC was performed to certify the infiltration of T cells in these two xenografts. The data showed that both GPC3-28Z T cells and GPC3-28Z-NFAT-IL-12 T cells could infiltrate into residual tumors, and there was significantly more $CD3^+$ T cell infiltration in tumors treated with GPC3-28Z-NFAT-IL-12 T cells

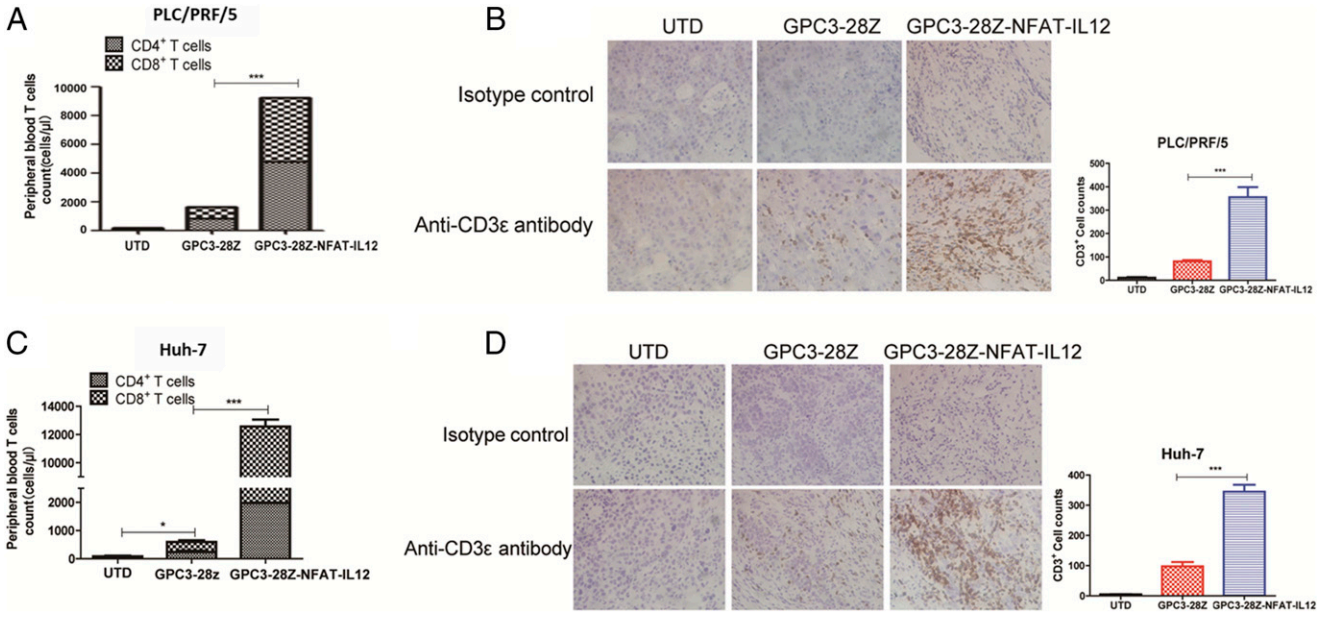

FIGURE 4. In vivo persistence and infiltration of GPC3-28Z-NFAT-IL-12 T cells. (**A** and **C**) The quantities of human T cells in peripheral blood from tumor-bearing mice treated with T cells 14 d after T cell infusion. Data shown are the mean ± SEM from three mice of each group. (**B** and **D**) The sections of formalin-fixed, paraffin-embedded tumor tissue from mice treated with indicated T cells were immunostained with anti-CD3ε Ab. The images were obtained under original magnification ×400. Data shown are from three independent experiments. $*p < 0.05$, $***p < 0.001$.

than with that treated with GPC3-28Z T cells (Fig. 4B, 4D). These results suggested that GPC3-28Z-NFAT-IL-12 T cells could inducibly express IL-12 in vivo, and IL-12 could favor the secretion of IFN-γ, the persistence and infiltration of CAR-T cells, and furthermore, augment antitumor activity of CAR-T cells.

Generation of murine GPC3-specific CAR-T cells releasing transgenic murine IL-12

To better understand the mechanisms in augmented antitumor efficacy of GPC3-28Z-NFAT-IL-12 T cells, further studies were carried out in immunocompetent mice models. We first constructed a murine second generation CAR. GPC3-m28Z is a chimeric receptor composed of the GPC3-targeting scFv (34) combined with murine CD28 and murine CD3ζ intracellular signaling domains (Fig. 5A, top panel). To further generate the murine IL-12–releasing CAR constructs, we fused GPC3-m28Z with a murine $NFAT_6$-IL-12-PA2 cassette to generate GPC3-m28Z-mNFAT-mIL-12 (Fig. 5A, bottom panel), which restricts murine IL-12 expression locally to tumor sites. Murine T cells were transduced retrovirally to express either GPC3-m28Z or GPC3-m28Z-mNFAT-mIL-12, and murine UTD (mUTD) cells served as controls. The transduction efficiency of murine CAR-T (mCAR-T) cells was then measured by FACS analysis 4 d post transduction (Fig. 5B).

Inducible expression of murine IL-12 and in vitro function of GPC3-m28Z-mNFAT-mIL-12 T cells

Hepa1-6 cells were lentivirally transduced with human mouse chimeric GPC3, designated as Hepa1-6-GPC3 (Fig. 5C). To test if murine IL-12 (mIL-12) secretion could be driven in an activation-dependent way, the mIL-12 secretion of CAR-T cells stimulated with Concanavalin A or GPC3-expressed target cells was tested after. The results showed that activated GPC3-m28Z-mNFAT-mIL-12 T cells expressed significantly more mIL-12 than that of in resting status, whereas no increased mIL-12 was observed in activated GPC3-m28Z T cells (Fig. 5D, Supplemental Fig. 1C). Meanwhile, we assessed the cytokine productions of murine CAR-T cells. The secretion of murine TNF-α (mTNF-α) and murine IFN-γ (mIFN-γ) were significantly higher in GPC3-m28Z-mNFAT-mIL-12 T cells compared with GPC3-m28Z T cells when cocultured with $GPC3^+$ tumor cells (Fig. 5E). However, we also found a markedly decreased amount of murine IL-2 (mIL-2) in GPC3-m28Z-mNFAT-mIL-12 T cells when cocultured with $GPC3^+$ tumor cells, which was coincident with previous studies demonstrating sensitization of T cells to IL-2 in the presence of IL-12 (44–46). However, we did not observe this phenomenon when human T cells (Fig. 2C). The cytotoxicity assay were also performed, and the data showed that GPC3-m28Z-mNFAT-mIL-12 T cells could kill $GPC3^+$ tumor cells equally effectively and specifically as GPC3-m28Z T cells (Fig. 5F).

Regression of large established tumors induced by GPC3-m28Z-mNFAT-mIL-12 T cells

To explore the antitumor efficacy of GPC3-m28Z-mNFAT-mIL-12 T cells in vivo, C57BL/6 mice were inoculated s.c. with Hepa1-6-GPC3 murine T cells transduced with GPC3-m28Z or GPC3-m28Z-mNFAT-mIL-12 at indicated doses and were infused without prior conditioning when tumors grew to 350–400 mm^3 (Fig. 6A). As shown in Fig. 6A, tumors in mice treated with GPC3-m28Z-mNFAT-mIL-12 T cells at both doses grew more slowly than those in mice treated with mUTD and GPC3-m28Z T cells. Mice were euthanized 24 d after T cell infusion, and the tumor-inhibiting rates of 2×10^6 GPC3-28Z T cells, 2×10^6, and 1×10^6 GPC3-28Z-NFAT-IL-12 T cells group were 6, 98, and 94%, respectively (Fig. 6B). We found that even GPC3-m28Z-mNFAT-mIL-12 T cells at a low dose (1×10^6) could mediate dramatic tumor regression, whereas GPC3-m28Z T cells at a high dose (2×10^6) failed to inhibit tumor growth. The inducible expression of mIL-12 did not resulted in obvious changes in body weight (Fig. 6C). In addition, there was no treatment-related injury observed (Supplemental Fig. 1D). Futher, the amounts of mIFN-γ and mIL-12 (p70) in sera were measured. Both mIFN-γ and mIL-12 were elevated in GPC3-m28Z-mNFAT-mIL-12 T cell–treated mice (at both doses) and barely detectable in mice treated with mUTD or GPC3-m28Z T cells (Fig. 6D). CAR copies in residual tumors were also detected. As Fig. 6E shows,

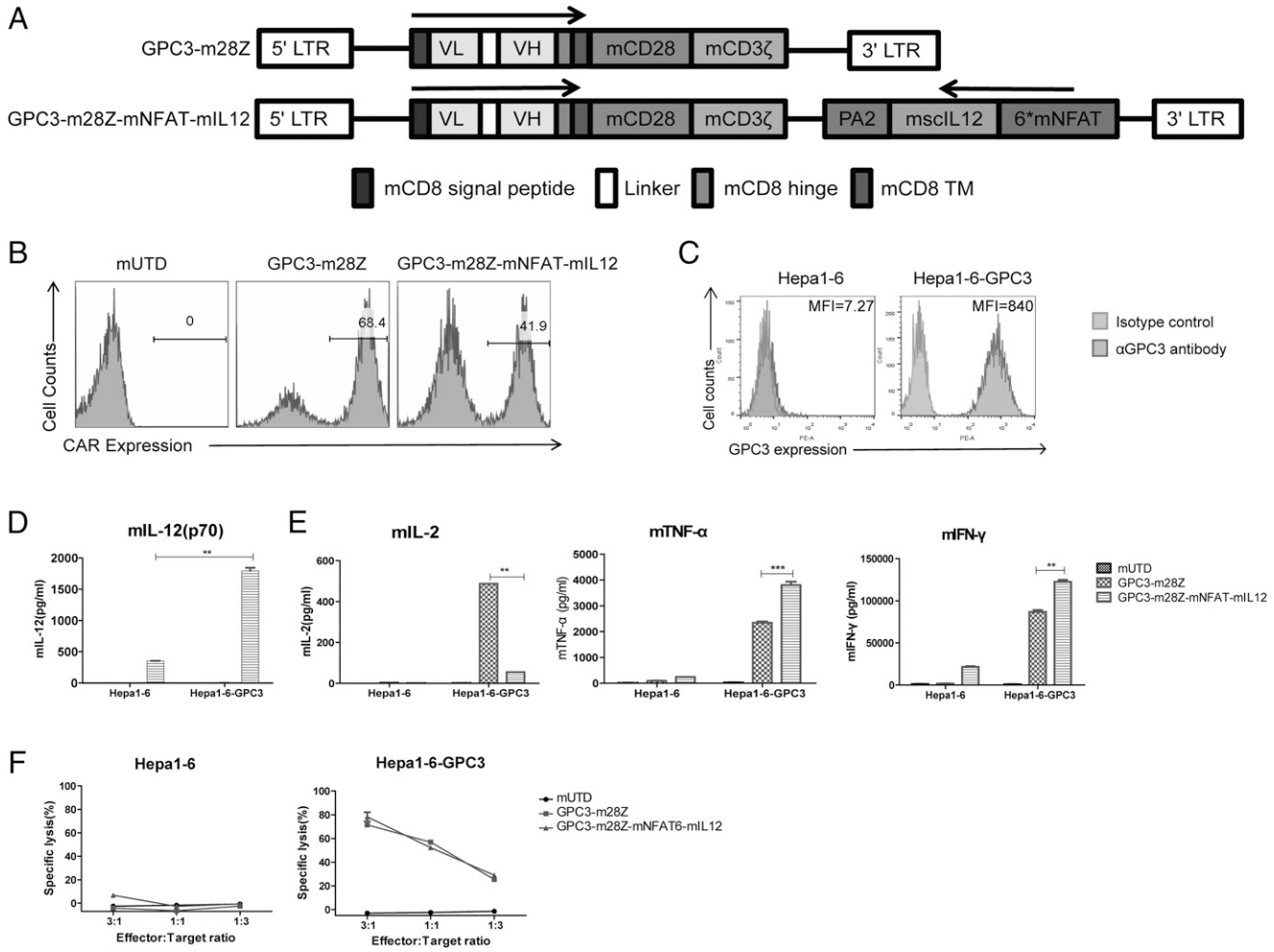

FIGURE 5. Murine GPC3-specific CARs construction and in vitro function of mCAR-T cells. (**A**) Schematic diagram of murine GPC3-CARs construction. (**B**) GPC3-CARs expression of murine CAR-T cells. The mUTD cells were used as controls. (**C**) GPC3 expression of murine tumor cells was determined by FACS. Isotype Ab served as a control. (**D** and **E**) The production of mIL-12 (p70), mIL-2, mTNF-α, and mIFN-γ of murine T cells after 24 h coculture with indicated tumor cells at 1:1 ratio was detected by ELISA. Data shown are the mean ± SEM of triplicates. (**F**) In vitro cytotoxicity of murine T cells incubated with indicated target cells at the indicated E:T ratios for 18 h. Each data set reflects mean ± SEM of quintuplicates. $^{**}p < 0.01$, $^{***}p < 0.001$.

the CAR copy numbers were more significantly elevated in the GPC3-m28Z-mNFAT-mIL-12 T cell group than those of in other groups. Previous studies reported the presence of $CD8^+$ T cells and a high CD8/Foxp3 ratio in solid tumors had a positive effect on survival (47). The infiltration of murine $CD8^+$ T cells and Tregs of tumor tissue were also assessed 8 d after murine T cell infusion. Compared with mUTD and GPC3-m28Z T cells, tumors in the GPC3-m28Z-mNFAT-mIL-12 T cell groups were infiltrated with more murine $CD8^+$ T cells and lower $Foxp3^+$ cells (Fig. 6F). Moreover, to investigate the antitumor efficacy of more, lower doses of murine CAR-T cells, 2×10^5, 5×10^5, and 1×10^6 GPC3-m28Z-mNFAT-mIL-12 T cells were transfused into mice bearing Hepa1-6-GPC3 xenografts. Interestingly, even the lowest dose of GPC3-m28Z-mNFAT-mIL-12 T cells (2×10^5) could also eradicate tumors (Supplemental Fig. 2A) 24 d after T cell infusion. To explore the kinetics of IL-12 expression after CAR-T infusion, the secretion of serum mIL-12 was detected. The results showed that the levels of serum mIL-12 gradually increased 12 d after GPC3-28Z-NFAT-IL-2-CAR-T infusion and then gradually reduced with the extension of CAR-T infusion (Supplemental Fig. 2B). These data indicated that mIL-12 accumulated at first and then decreased along with the tumors being eradicated. Furthermore, we also measured the IL-12 levels in the sera of mice not bearing tumors. The results showed that there was almost no IL-12 secretion observed in the serum of UTD-, GPC3-m28Z–, and GPC3-m28Z-mNFAT-mIL-12 T cell–treated mice (Supplemental Fig. 2C). These data suggested the GPC3-specific on-tumor activation of the NFAT-IL-12 cassette in GPC3-28Z-NFAT-IL-2-CAR-T cells. Collectively, our results demonstrated that in vivo GPC3-m28Z-mNFAT-mIL-12 T cells could be induced to secrete mIL-12, which could augment mIFN-γ secretion, increase murine $CD8^+$ T cells infiltration, decrease murine Treg infiltration, and further augment antitumor immunity when used against $GPC3^+$ HCC tumors.

Discussion

Adoptive immunotherapy based on CAR-T cells has been demonstrated as a promising strategy in B cell lymphoid malignancies. However, this clinical success has failed to translate into solid tumors to a large extent because of the heterogeneity of tumor cells and the hostile tumor microenvironment, which involves inhibitory cells, such as myeloid-derived suppressor cells, Tregs, and immunosuppressive cytokines, such as IL-10, as well as immune checkpoint molecules, such as PD-L1 (48, 49). These obstacles limit the proliferation and persistence of CAR-T cells and, furthermore, tend to impair the antitumor efficiency of CAR-T cells.

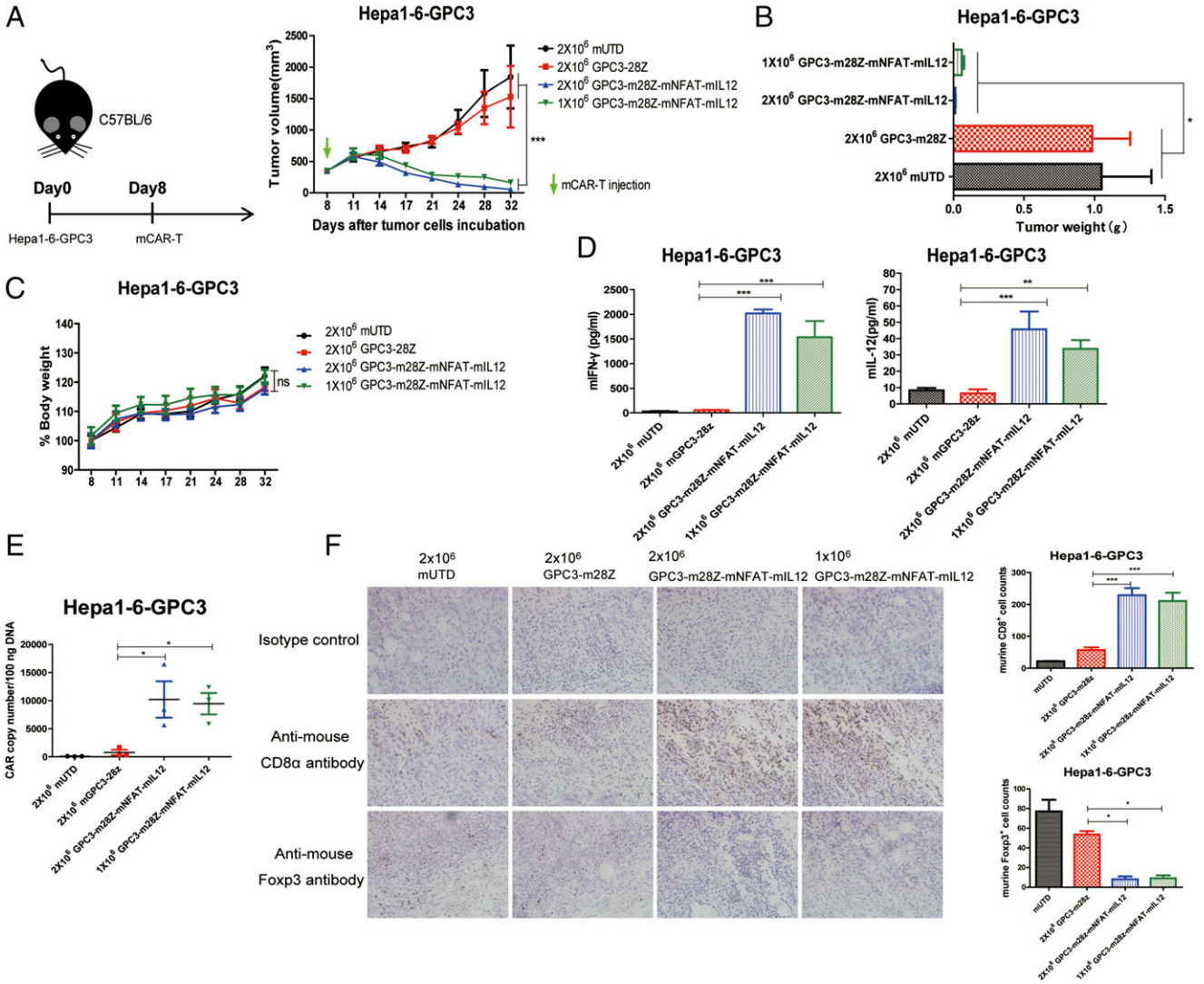

FIGURE 6. GPC3-m28Z-mNFAT-mIL-12 T cells improved antitumor immunity against established murine HCC tumor. (**A**) Left panel, Experimental scheme of in vivo immunocompetent model. Murine T cells at different doses were transferred i.v. into female C57BL/6 mice 8 d after tumor cell inoculation ($n = 6$). Right panel, Tumor growth curve for Hepa1-6-GPC3 xenografts treated with indicated murine T cells. Arrow indicates murine T cells infusion. (**B**) The tumor weight was measured at the study end point. (**C**) Body weight of each group was measured every 3–4 d (baseline = 100%). (**D**) The amounts of mIFN-γ and mIL-12 (p70) in the sera of treated mice 8 d after therapy were assessed by ELISA. Data shown are the mean ± SEM. (**E**) CAR copy numbers in genomic DNA of residual tumors 8 d after therapy were measured by real-time PCR. (**F**) The sections of formalin-fixed, paraffin-embedded tumor tissue were immunostained with anti-mouse CD8α Ab or anti-mouse Foxp3 Ab. The images were obtained under original magnification ×400. Data shown are from three independent experiments. $^*p < 0.05$, $^{**}p < 0.01$, $^{***}p < 0.001$.

IL-12 is a heterodimeric proinflammatory cytokine mainly produced by APCs such as dendritic cells and macrophages (50). Given its potent mobilization of the immune systems, IL-12 has emerged as one of the most robust cytokines in mediating antitumor activity in various murine tumor models (18, 51, 52). Brunda and colleagues (53) demonstrated rIL-12 exerted antitumor responses in murine models. However, much evidence has demonstrated that systemic administration of rIL-12 could bring some severe toxicities, including deaths, which extremely restricted its clinical application (24, 25). Thus, some researchers attempted to localize the effects of IL-12 into the tumor environment (54–56) or express IL-12 locally via different gene therapy vectors (57–59). Although monotherapy of IL-12 showed limited therapeutic effects, the compelling antitumor properties of IL-12 made it a promising candidate for combination with other therapeutic strategies. Wagner and colleagues (60) first reported a local delivery of IL-12 to tumor sites by EBV-specific cytotoxic T cells. Subsequently, researchers have launched various preclinical and clinical studies using different effector cells, such as tumor-infiltrating lymphocytes and CAR-T cells, with either constitutive or inducible expression of IL-12 (37, 61).

In this study, we combined GPC3-specific CAR-T cells with inducible IL-12 expression and explored antitumor efficacy of CAR-T cells in immunodeficient and immunocompetent hosts. The results showed the activation-dependent production of IL-12 in GPC3-28Z-NFAT-IL-12 T cells when cocultured with target cells in vitro. GPC3-28Z T cells and GPC3-28Z-NFAT-IL-12 T cells lysed $GPC3^+$ tumor cells with equal efficiency, which suggested that the transgene of IL-12 did not compromise the cytotoxicity of CAR-T cells. However, even with similar cytotoxicity, GPC3-28Z-NFAT-IL-12 T cells displayed augmented cytokine secretion compared with GPC3-28Z T cells. In vivo, GPC3-28Z-NFAT-IL-12 T cells were more potent when applied against GPC3-expression tumors without obvious toxicity compared with GPC3-28Z T cells, which could be attributed to IL-12 favoring IFN-γ production and the infiltration and persistence of CAR-T cells. There is a concern

that better infiltration and persistence of CAR-T cells might incur potential unwanted side effects, such as off-tumor toxicity. The infiltration of CAR-T cells was also measured in mice liver tissues, and no human $CD3^+$ T cells were observed in liver tissues (Supplemental Fig. 1B). In immunocompetent mice, GPC3-m28Z-mNFAT-mIL-12 T cells showed the more cytokine secretion and similar cytotoxicity compared with GPC3-m28Z T cells in vitro. In vivo, GPC3-m28Z-mNFAT-mIL-12 T cells augmented antitumor immunity without the need for prior conditioning, which could be attributed to mIL-12 increasing mIFN-γ production, favoring murine $CD8^+$ T cell infiltration into established tumors. Strikingly, decreasing the dose of CAR-T cells could also achieve remarkable antitumor efficacy. In addition, releasing mIL-12 decreased Treg frequency in established tumors, as previous studies reported (62, 63), which paved the way for CAR-T cells performing an antitumor function in a hostile tumor microenvironment.

Nevertheless, our study also has some limitations. The mice models used in this study were not suitable to assess toxicity because the CAR-T cells are specific for a human Ag. It was difficult to observe the on-target off-tumor effects in our animal experiments. Additionally, we did not use orthotopic tumor models to investigate the antitumor efficacy and toxicity of CAR-T cells in vivo. It is unknown if toxicity would be greater in situ than s.c., so deeper studies are needed for further investigation before GPC3-28Z-NFAT-IL-12 T cells are translated into clinical application.

Together, our research demonstrated the inducible expression of IL-12 could boost CAR-T cell function with less potential side effects, both in immunodeficient and immunocompetent hosts, and the combination of CAR-T therapy with IL-12 makes it possible to decrease the application dose of CAR-T cells, which is of great significance to cancer patients with damaged T lymphocytes. These findings may broaden the application of CAR-T–based immunotherapy to patients intolerant of lymphodepletion chemotherapy and might be an alternative therapeutic strategy for patients suffering from low GPC3-expression HCC or advanced large $GPC3^+$ HCC and other $GPC3^+$ solid tumors.

Disclosures

Z.L. has ownership interests in GPC3-specific CAR-T cells and has filed patents related to GPC3 CAR-T cells. The other authors have no financial conflicts of interest.

References

1. El-Serag, H. B., and K. L. Rudolph. 2007. Hepatocellular carcinoma: epidemiology and molecular carcinogenesis. *Gastroenterology* 132: 2557–2576.
2. Altekruse, S. F., K. A. McGlynn, and M. E. Reichman. 2009. Hepatocellular carcinoma incidence, mortality, and survival trends in the United States from 1975 to 2005. *J. Clin. Oncol.* 27: 1485–1491.
3. Clavien, P. A., H. Petrowsky, M. L. DeOliveira, and R. Graf. 2007. Strategies for safer liver surgery and partial liver transplantation. *N. Engl. J. Med.* 356: 1545–1559.
4. Raza, A., and G. K. Sood. 2014. Hepatocellular carcinoma review: current treatment, and evidence-based medicine. *World J. Gastroenterol.* 20: 4115–4127.
5. Couzin-Frankel, J. 2013. Breakthrough of the year 2013. Cancer immunotherapy. *Science* 342: 1432–1433.
6. Grupp, S. A., M. Kalos, D. Barrett, R. Aplenc, D. L. Porter, S. R. Rheingold, D. T. Teachey, A. Chew, B. Hauck, J. F. Wright, et al. 2013. Chimeric antigen receptor-modified T cells for acute lymphoid leukemia. *N. Engl. J. Med.* 368: 1509–1518.
7. Davila, M. L., I. Riviere, X. Wang, S. Bartido, J. Park, K. Curran, S. S. Chung, J. Stefanski, O. Borquez-Ojeda, M. Olszewska, et al. 2014. Efficacy and toxicity management of 19-28z CAR T cell therapy in B cell acute lymphoblastic leukemia. *Sci. Transl. Med.* 6: 224ra25.
8. Gill, S., and C. H. June. 2015. Going viral: chimeric antigen receptor T-cell therapy for hematological malignancies. *Immunol. Rev.* 263: 68–89.
9. Maude, S. L., N. Frey, P. A. Shaw, R. Aplenc, D. M. Barrett, N. J. Bunin, A. Chew, V. E. Gonzalez, Z. Zheng, S. F. Lacey, et al. 2014. Chimeric antigen receptor T cells for sustained remissions in leukemia. *N. Engl. J. Med.* 371: 1507–1517.
10. Lamers, C. H., S. Sleijfer, S. van Steenbergen, P. van Elzakker, B. van Krimpen, C. Groot, A. Vulto, M. den Bakker, E. Oosterwijk, R. Debets, and J. W. Gratama. 2013. Treatment of metastatic renal cell carcinoma with CAIX CAR-engineered T cells: clinical evaluation and management of on-target toxicity. *Mol. Ther.* 21: 904–912.
11. Beatty, G. L., and M. O'Hara. 2016. Chimeric antigen receptor-modified T cells for the treatment of solid tumors: defining the challenges and next steps. *Pharmacol. Ther.* 166: 30–39.
12. Feng, K., Y. Liu, Y. Guo, J. Qiu, Z. Wu, H. Dai, Q. Yang, Y. Wang, and W. Han. 2017. Phase I study of chimeric antigen receptor modified T cells in treating HER2-positive advanced biliary tract cancers and pancreatic cancers. *Protein Cell* 9: 838–847.
13. Ahmed, N., V. S. Brawley, M. Hegde, C. Robertson, A. Ghazi, C. Gerken, E. Liu, O. Dakhova, A. Ashoori, A. Corder, et al. 2015. Human epidermal growth factor receptor 2 (HER2) -specific chimeric antigen receptor-modified T cells for the immunotherapy of HER2-positive sarcoma. *J. Clin. Oncol.* 33: 1688–1696.
14. Beatty, G. L., A. R. Haas, M. V. Maus, D. A. Torigian, M. C. Soulen, G. Plesa, A. Chew, Y. Zhao, B. L. Levine, S. M. Albelda, et al. 2014. Mesothelin-specific chimeric antigen receptor mRNA-engineered T cells induce anti-tumor activity in solid malignancies. *Cancer Immunol. Res.* 2: 112–120.
15. Scarfò, I., and M. V. Maus. 2017. Current approaches to increase CAR T cell potency in solid tumors: targeting the tumor microenvironment. *J. Immunother. Cancer* 5: 28.
16. Sadelain, M., R. Brentjens, and I. Rivière. 2013. The basic principles of chimeric antigen receptor design. *Cancer Discov.* 3: 388–398.
17. Yeku, O. O., and R. J. Brentjens. 2016. Armored CAR T-cells: utilizing cytokines and pro-inflammatory ligands to enhance CAR T-cell anti-tumour efficacy. *Biochem. Soc. Trans.* 44: 412–418.
18. Trinchieri, G. 2003. Interleukin-12 and the regulation of innate resistance and adaptive immunity. *Nat. Rev. Immunol.* 3: 133–146.
19. Curtsinger, J. M., D. C. Lins, and M. F. Mescher. 2003. Signal 3 determines tolerance versus full activation of naive CD8 T cells: dissociating proliferation and development of effector function. *J. Exp. Med.* 197: 1141–1151.
20. Ma, X., J. M. Chow, G. Gri, G. Carra, F. Gerosa, S. F. Wolf, R. Dzialo, and G. Trinchieri. 1996. The interleukin 12 p40 gene promoter is primed by interferon gamma in monocytic cells. *J. Exp. Med.* 183: 147–157.
21. Chan, S. H., B. Perussia, J. W. Gupta, M. Kobayashi, M. Pospísil, H. A. Young, S. F. Wolf, D. Young, S. C. Clark, and G. Trinchieri. 1991. Induction of interferon gamma production by natural killer cell stimulatory factor: characterization of the responder cells and synergy with other inducers. *J. Exp. Med.* 173: 869–879.
22. Kerkar, S. P., R. S. Goldszmid, P. Muranski, D. Chinnasamy, Z. Yu, R. N. Reger, A. J. Leonardi, R. A. Morgan, E. Wang, F. M. Marincola, et al. 2011. IL-12 triggers a programmatic change in dysfunctional myeloid-derived cells within mouse tumors. *J. Clin. Invest.* 121: 4746–4757.
23. Tahara, H., L. Zitvogel, W. J. Storkus, P. D. Robbins, and M. T. Lotze. 1996. Murine models of cancer cytokine gene therapy using interleukin-12. *Ann. N. Y. Acad. Sci.* 795: 275–283.
24. Leonard, J. P., M. L. Sherman, G. L. Fisher, L. J. Buchanan, G. Larsen, M. B. Atkins, J. A. Sosman, J. P. Dutcher, N. J. Vogelzang, and J. L. Ryan. 1997. Effects of single-dose interleukin-12 exposure on interleukin-12-associated toxicity and interferon-gamma production. *Blood* 90: 2541–2548.
25. Cohen, J. 1995. IL-12 deaths: explanation and a puzzle. *Science* 270: 908.
26. Koneru, M., T. J. Purdon, D. Spriggs, S. Koneru, and R. J. Brentjens. 2015. IL-12 secreting tumor-targeted chimeric antigen receptor T cells eradicate ovarian tumors *in vivo*. *OncoImmunology* 4: e994446.
27. Chinnasamy, D., Z. Yu, S. P. Kerkar, L. Zhang, R. A. Morgan, N. P. Restifo, and S. A. Rosenberg. 2012. Local delivery of interleukin-12 using T cells targeting VEGF receptor-2 eradicates multiple vascularized tumors in mice. *Clin. Cancer. Res.* 18: 1672–1683.
28. Haruyama, Y., and H. Kataoka. 2016. Glypican-3 is a prognostic factor and an immunotherapeutic target in hepatocellular carcinoma. *World J. Gastroenterol.* 22: 275–283.
29. Zhu, A. X., P. J. Gold, A. B. El-Khoueiry, T. A. Abrams, H. Morikawa, N. Ohishi, T. Ohtomo, and P. A. Philip. 2013. First-in-man phase I study of GC33, a novel recombinant humanized antibody against glypican-3, in patients with advanced hepatocellular carcinoma. *Clin. Cancer. Res.* 19: 920–928
30. Ikeda, M., S. Ohkawa, T. Okusaka, S. Mitsunaga, S. Kobayashi, C. Morizane, I. Suzuki, S. Yamamoto, and J. Furuse. 2014. Japanese phase I study of GC33, a humanized antibody against glypican-3 for advanced hepatocellular carcinoma. *Cancer Sci.* 105: 455–462.
31. Sawada, Y., T. Yoshikawa, D. Nobuoka, H. Shirakawa, T. Kuronuma, Y. Motomura, S. Mizuno, H. Ishii, K. Nakachi, M. Konishi, et al. 2012. Phase I trial of a glypican-3-derived peptide vaccine for advanced hepatocellular carcinoma: immunologic evidence and potential for improving overall survival. *Clin. Cancer. Res.* 18: 3686–3696.
32. Zhai, B., D. Shi, H. Gao, X. Qi, H. Jiang, Y. Zhang, J. Chi, H. Ruan, H. Wang, Q. C. Ru, and Z. Li. 2017. A phase I study of anti-GPC3 chimeric antigen receptor modified T cells (GPC3 CAR-T) in Chinese patients with refractory or relapsed GPC3+ hepatocellular carcinoma (r/r GPC3+ HCC). *J. Clin. Oncol.* 35(15_Suppl.): 3049.
33. Zhou, F., W. Shang, and X. Yu. 2018. Glypican-3: A promising biomarker for hepatocellular carcinoma diagnosis and treatment. *Med. Res. Rev.* 38: 741–767.
34. Bi, Y., H. Jiang, P. Wang, B. Song, H. Wang, X. Kong, and Z. Li. 2017. Treatment of hepatocellular carcinoma with a GPC3-targeted bispecific T cell engager. *Oncotarget* 8: 52866–52876.
35. Gao, H., K. Li, H. Tu, X. Pan, H. Jiang, B. Shi, J. Kong, H. Wang, S. Yang, J. Gu, and Z. Li. 2014. Development of T cells redirected to glypican-3 for the treatment of hepatocellular carcinoma. *Clin. Cancer. Res.* 20: 6418–6428

36. Jiang, H., B. Song, P. Wang, B. Shi, Q. Li, M. Fan, S. Di, J. Yang, and Z. Li. 2017. Efficient growth suppression in pancreatic cancer PDX model by fully human anti-mesothelin CAR-T cells. *Protein Cell.* 8: 926–931.
37. Zhang, L., S. P. Kerkar, Z. Yu, Z. Zheng, S. Yang, N. P. Restifo, S. A. Rosenberg, and R. A. Morgan. 2011. Improving adoptive T cell therapy by targeting and controlling IL-12 expression to the tumor environment. *Mol. Ther.* 19: 751–759.
38. Hooijberg, E., A. Q. Bakker, J. J. Ruizendaal, and H. Spits. 2000. NFAT-controlled expression of GFP permits visualization and isolation of antigen-stimulated primary human T cells. *Blood* 96: 459–466.
39. Kerkar, S. P., P. Muranski, A. Kaiser, A. Boni, L. Sanchez-Perez, Z. Yu, D. C. Palmer, R. N. Reger, Z. A. Borman, L. Zhang, et al. 2010. Tumor-specific CD8+ T cells expressing interleukin-12 eradicate established cancers in lymphodepleted hosts. *Cancer Res.* 70: 6725–6734.
40. Chinnasamy, D., Z. Yu, M. R. Theoret, Y. Zhao, R. K. Shrimali, R. A. Morgan, S. A. Feldman, N. P. Restifo, and S. A. Rosenberg. 2010. Gene therapy using genetically modified lymphocytes targeting VEGFR-2 inhibits the growth of vascularized syngenic tumors in mice. *J. Clin. Invest.* 120: 3953–3968.
41. Longo, P. A., J. M. Kavran, M. S. Kim, and D. J. Leahy. 2013. Transient mammalian cell transfection with polyethylenimine (PEI). *Methods Enzymol.* 529: 227–240.
42. Kuroda, H., R. H. Kutner, N. G. Bazan, and J. Reiser. 2009. Simplified lentivirus vector production in protein-free media using polyethylenimine-mediated transfection. *J. Virol. Methods* 157: 113–121.
43. Li, K., X. Pan, Y. Bi, W. Xu, C. Chen, H. Gao, B. Shi, H. Jiang, S. Yang, L. Jiang, and Z. Li. 2016. Adoptive immunotherapy using T lymphocytes redirected to glypican-3 for the treatment of lung squamous cell carcinoma. *Oncotarget* 7: 2496–2507.
44. Pegram, H. J., J. C. Lee, E. G. Hayman, G. H. Imperato, T. F. Tedder, M. Sadelain, and R. J. Brentjens. 2012. Tumor-targeted T cells modified to secrete IL-12 eradicate systemic tumors without need for prior conditioning. *Blood* 119: 4133–4141.
45. Yeku, O. O., T. J. Purdon, M. Koneru, D. Spriggs, and R. J. Brentjens. 2017. Armored CAR T cells enhance antitumor efficacy and overcome the tumor microenvironment. *Sci. Rep.* 7: 10541.
46. Lisiero, D. N., H. Soto, L. M. Liau, and R. M. Prins. 2011. Enhanced sensitivity to IL-2 signaling regulates the clinical responsiveness of IL-12-primed CD8(+) T cells in a melanoma model. *J. Immunol.* 186: 5068–5077.
47. Hadrup, S., M. Donia, and P. Thor Straten. 2013. Effector CD4 and CD8 T cells and their role in the tumor microenvironment. *Cancer Microenviron.* 6: 123–133.
48. Yu, S., A. Li, Q. Liu, T. Li, X. Yuan, X. Han, and K. Wu. 2017. Chimeric antigen receptor T cells: a novel therapy for solid tumors. *J. Hematol. Oncol.* 10: 78.
49. Marigo, I., L. Dolcetti, P. Serafini, P. Zanovello, and V. Bronte. 2008. Tumor-induced tolerance and immune suppression by myeloid derived suppressor cells. *Immunol. Rev.* 222: 162–179.
50. Trinchieri, G., M. Rengaraju, A. D'Andrea, N. M. Valiante, M. Kubin, M. Aste, and J. Chehimi. 1993. Producer cells of interleukin-12. *Immunol. Today* 14: 237–238.
51. Tugues, S., S. H. Burkhard, I. Ohs, M. Vrohlings, K. Nussbaum, J. Vom Berg, P. Kulig, and B. Becher. 2015. New insights into IL-12-mediated tumor suppression. *Cell Death Differ.* 22: 237–246.
52. Hendrzak, J. A., and M. J. Brunda. 1996. Antitumor and antimetastatic activity of interleukin-12. *Curr. Top. Microbiol. Immunol.* 213: 65–83.
53. Brunda, M. J., L. Luistro, R. R. Warrier, R. B. Wright, B. R. Hubbard, M. Murphy, S. F. Wolf, and M. K. Gately. 1993. Antitumor and antimetastatic activity of interleukin 12 against murine tumors. *J. Exp. Med.* 178: 1223–1230.
54. Halin, C., S. Rondini, F. Nilsson, A. Berndt, H. Kosmehl, L. Zardi, and D. Neri. 2002. Enhancement of the antitumor activity of interleukin-12 by targeted delivery to neovasculature. *Nat. Biotechnol.* 20: 264–269.
55. Peng, L. S., M. L. Penichet, and S. L. Morrison. 1999. A single-chain IL-12 IgG3 antibody fusion protein retains antibody specificity and IL-12 bioactivity and demonstrates antitumor activity. *J. Immunol.* 163: 250–258.
56. Dickerson, E. B., N. Akhtar, H. Steinberg, Z. Y. Wang, M. J. Lindstrom, M. L. Padilla, R. Auerbach, and S. C. Helfand. 2004. Enhancement of the antiangiogenic activity of interleukin-12 by peptide targeted delivery of the cytokine to alphavbeta3 integrin. *Mol. Cancer Res.* 2: 663–673.
57. Heinzerling, L., G. Burg, R. Dummer, T. Maier, P. A. Oberholzer, J. Schultz, L. Elzaouk, J. Pavlovic, and K. Moelling. 2005. Intratumoral injection of DNA encoding human interleukin 12 into patients with metastatic melanoma: clinical efficacy. *Hum. Gene Ther.* 16: 35–48.
58. Mahvi, D. M., M. B. Henry, M. R. Albertini, S. Weber, K. Meredith, H. Schalch, A. Rakhmilevich, J. Hank, and P. Sondel. 2007. Intratumoral injection of IL-12 plasmid DNA--results of a phase I/IB clinical trial. *Cancer Gene Ther.* 14: 717–723.
59. Daud, A. I., R. C. DeConti, S. Andrews, P. Urbas, A. I. Riker, V. K. Sondak, P. N. Munster, D. M. Sullivan, K. E. Ugen, J. L. Messina, and R. Heller. 2008. Phase I trial of interleukin-12 plasmid electroporation in patients with metastatic melanoma. *J. Clin. Oncol.* 26: 5896–5903.
60. Wagner, H. J., C. M. Bollard, S. Vigouroux, M. H. Huls, R. Anderson, H. G. Prentice, M. K. Brenner, H. E. Heslop, and C. M. Rooney. 2004. A strategy for treatment of Epstein-Barr virus-positive Hodgkin's disease by targeting interleukin 12 to the tumor environment using tumor antigen-specific T cells. *Cancer Gene Ther.* 11: 81–91.
61. Zhang, L., R. A. Morgan, J. D. Beane, Z. Zheng, M. E. Dudley, S. H. Kassim, A. V. Nahvi, L. T. Ngo, R. M. Sherry, G. Q. Phan, et al. 2015. Tumor-infiltrating lymphocytes genetically engineered with an inducible gene encoding interleukin-12 for the immunotherapy of metastatic melanoma. *Clin. Cancer. Res.* 21: 2278–2288.
62. Chmielewski, M., and H. Abken. 2017. CAR T cells releasing IL-18 convert to T-Bet^{high} FoxO1^{low} effectors that exhibit augmented activity against advanced solid tumors. *Cell Reports* 21: 3205–3219.
63. Shi, G., C. Edelblute, C. Lundberg, and R. Heller. 2017. Intratumoral IL-12 gene electrotransfer-mediated regression of established B16F10 melanoma protects against rechallenge. *J. Immunol.* 198(1 Supplement): 126.10.

Armored Inducible Expression of IL-12 enhances Antitumor Activity of Glypican-3-targeted chimeric antigen receptor engineered T cells in Hepatocellular carcinoma

Supplementary materials:

Supplementary Figure. 1

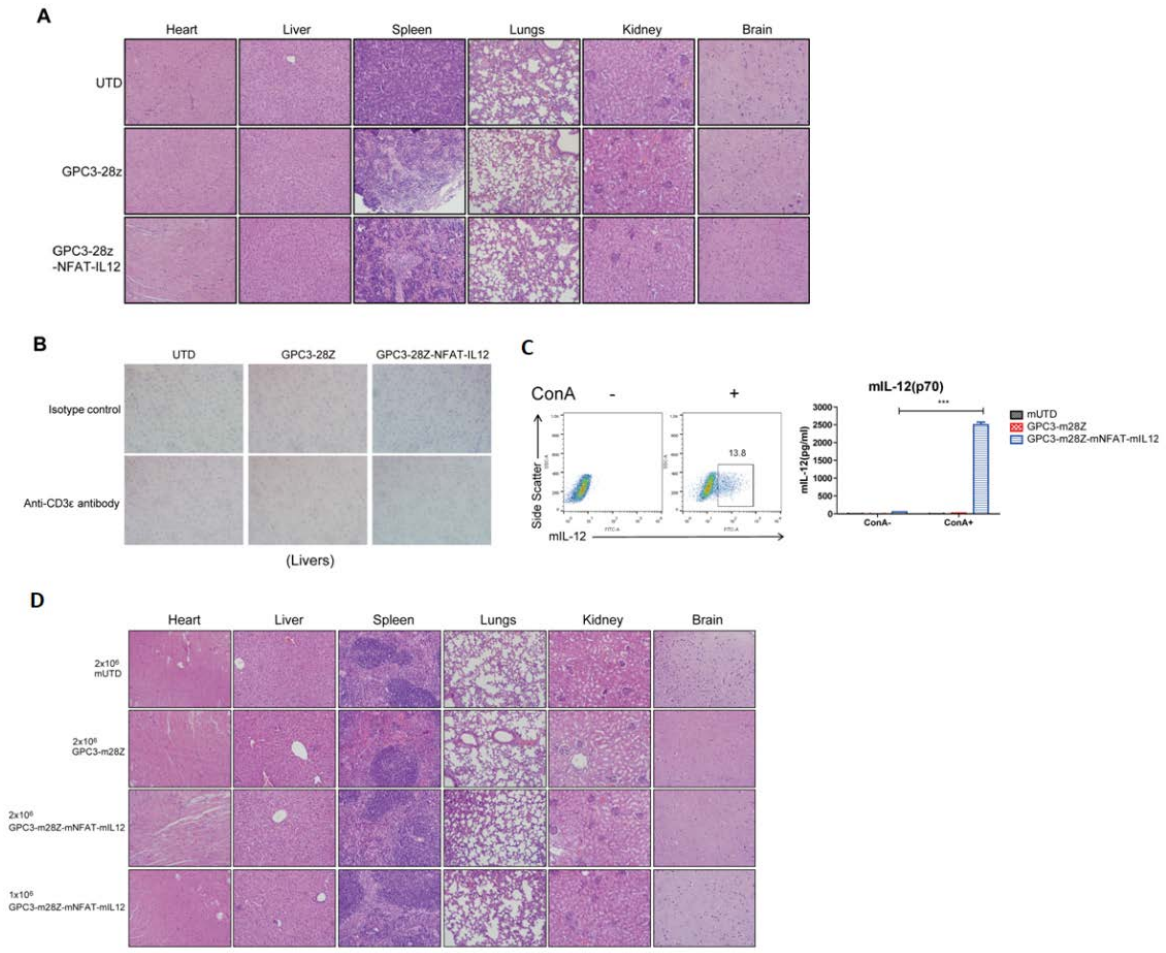

Supplementary Figure 1

A, representative haematoxylin and eosin-stained sections of various organs derived from NSG mice bearing Huh-7 xenografts after 10 days treated with UTD, GPC3-28Z and GPC3-28Z-NFAT-IL12 T cells. The images were obtained under 200× magnification. B, the sections of formalin-fixed paraffin-embedded livers from Huh-7-xenografts-bearing mice 25 days post treated with indicated T cells were immunostained with anti-CD3ε antibody. The images were obtained under 400× magnification. C, left panel: the expression of murine IL-12 in GPC3-m28Z-mNFAT-mIL12 T cells with or without Concanavalin A (ConA, 10μg/ml) stimulation. Right panel: the secretion of mIL-12p70 from murine T cells following overnight stimulation with ConA was measured by ELISA. Data shown is the mean±SEM of triplicates. D, representative haematoxylin and eosin-stained sections of various organs derived from C57BL/6 mice bearing Hepa1-6-GPC3 xenografts after 8 days treated with indicated murine T cells. The images were obtained under 200× magnification.

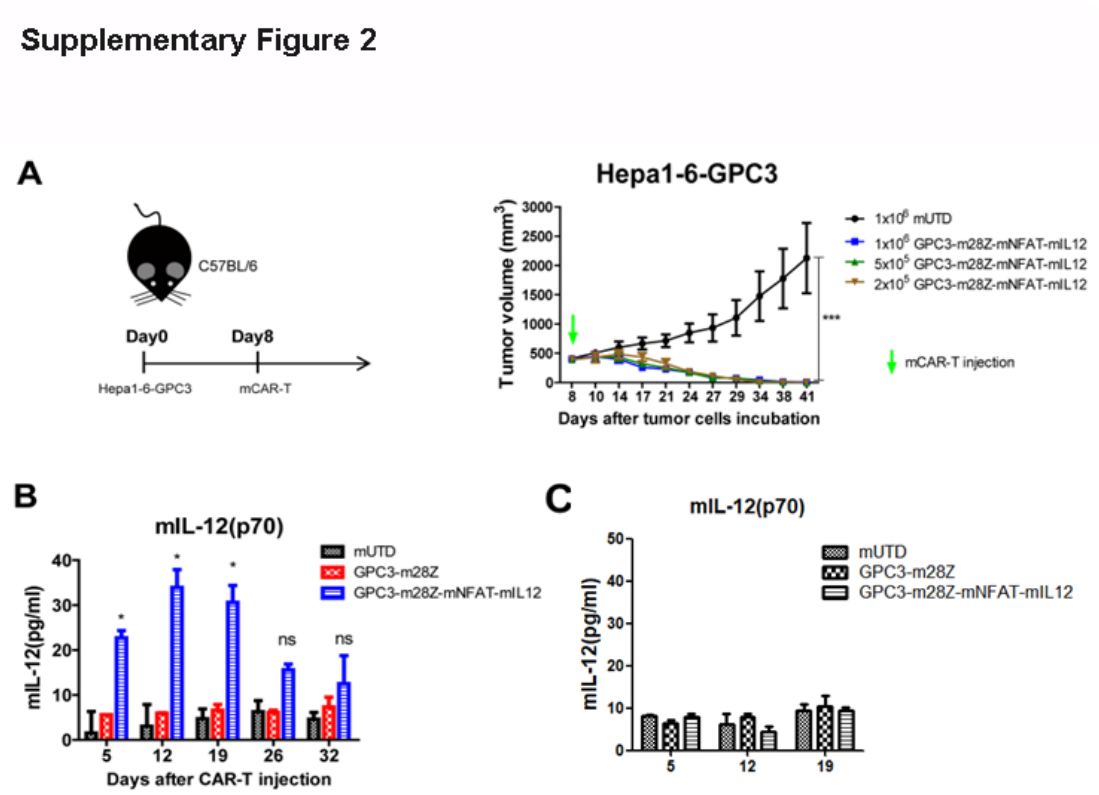

Supplementary Figure 2

A, the antitumor efficacy of lower doses of GPC3-m28Z-mNFAT-mIL12 T cells.Hepa1-6-GPC3 xenografts were established subcutaneously on the right flanks of 6-week-old female C57BL/6 mice (n=6). Murine T cells at different doses (1×10^6, 5×10^5 and 2×10^5) were transfused into mice 8 days post tumor cells inoculation. Green Arrow indicated murine T cells infusion. B, the murine serum on day 5, 12, 19, 26, 32 after T cells injection was collected and the mIL-12expression was dynamically detected by ELISA after murine T cells infusion. C, the mIL-12 secretion was measured in the sera of mice without bearing tumors by ELISA after murine T cells infusion.